# **Electrospinning of Colloidal Mixture of Oxide Nanoparticles for Transparent and Conductive Films**

# Minjun LEE<sup>1</sup>, Jae-Hun CHUNG<sup>1</sup>, Young Seok KIM<sup>2</sup>, Young-Sang CHO<sup>1\*</sup>

http://doi.org/10.5755/j02.ms.39977

Received 1 January 2025; accepted 8 April 2025

This study addresses the research to overcome the cost disadvantages of indium tin oxide (ITO) by using antimony-doped tin oxide (ATO) as an alternative to transparent conductive films. ITO contains indium, a rare metal, making it expensive and mechanically fragile. On the other hand, ATO is inexpensive, stable, and has excellent electrical and mechanical properties. The main objective of the study is to optimize the mixing ratio of ATO and ITO to maintain conductivity and transparency and solve cost issues. ATO and ITO nanoparticle colloids were prepared using a wet attrition method and electrospun on glass substrates at various mixing ratios to form transparent conductive films. Increasing electrospinning time and increasing ITO concentration contributed to the decrease in surface resistance, and when acetylacetone was used as a dispersant, the heat treatment process resulted in lower surface resistance. When the sintering temperature was between 400 °C and 550 °C, the removal of organic components was accelerated and the surface resistance decreased. This shows the importance of network formation of conductive nanoparticles through stable high-temperature sintering and the adoption of suitable dispersants. This study presents the possibility of manufacturing cost-effective transparent conductive films through ATO and ITO mixing ratios. The results of these technologies and research can contribute to reducing costs and improving performance during the display production process.

Keywords: antimony tin oxide, indium tin oxide, electrospinning, transparent electrode, nano-colloid, wet grinding.

## 1. INTRODUCTION

ITO (Indium Tin Oxide) is a highly conductive material used in the production of transparent thin films commonly applied in touch screen panels. However, concerns regarding resource availability and cost have been raised due to indium being classified as a rare metal, and the mechanical fragility of this material is also becoming a significant issue [1]. Additionally, more than half of the world's indium production occurs in China, and the price of indium has risen over the past decade. Consequently, various studies are being conducted to find alternatives to the expensive ITO [2]. To address these issues, relatively inexpensive and highly resistive ATO (Antimony-doped Tin Oxide) has been proposed as an alternative. ATO offers not only cost advantages but also electrical and mechanical properties, as well as excellent thermal and environmental stability [3-9]. This study aims to find sufficient resistivity values by mixing ATO as a potential replacement for ITO.

Currently, transparent conductive materials are used in devices such as flat panel displays and solar cells [3]. Due to the need for options that are lightweight, flexible, cost-effective, and capable of mass production, demand for such materials is increasing. Consequently, the disadvantages of ITO, which relies on the rare earth element indium, have become more pronounced, highlighting the urgent need for alternative materials. Cost reduction in the rapidly evolving transparent electrode market is crucial for maintaining market competitiveness. Over the years, new materials such

as conductive polymers and carbon nanotubes, as well as innovative manufacturing methods, have been developed to address these issues [10-15]. However, there are still significant limitations in completely replacing ITO.

Due to its limitations, ITO, which is the primary material for transparent conductive films, presents various challenges for direct use. As a result, there are numerous global research efforts underway to address these issues. One approach involves mitigating the drawbacks of ITO by complementing it with other materials to some extent [16]. Another approach focuses on developing technologies using materials that can completely replace ITO [17-18]. Additionally, research is also exploring biodegradable and biocompatible materials to reduce electronic waste and enhance applications in electronics [19].

Transparent conductive films, essential for screens of various electronic products like rollable, foldable, and stretchable devices, are garnering significant interest [20]. These features and related technologies are expected to have a substantial economic impact, especially in applications such as wearable devices and transparent solar panels. However, the high cost of ITO, influenced by international markets and political factors due to the rare earth metal indium, poses a burden on product manufacturing and sales.

This study aims to manufacture transparent conductive films by mixing ITO and ATO solutions, which have been individually reported in numerous cases, and evaluate the electrical and optical properties of the films based on dispersant type, chemical stoichiometry ratio, injection

<sup>&</sup>lt;sup>1</sup> Department of Chemical Engineering and Biotechnology, Tech University of Korea, 237, Siheung-si, Gyeonggi-do 15073, Republic of Korea

<sup>&</sup>lt;sup>2</sup> Display Components & Materials Research Center, Korea Electronics Technology Institute, 68 Yatap, Bundang, Seongnam-si, Gyeonggi-do, Korea

<sup>\*</sup> Corresponding author. Y.-S. Cho E-mail: yscho78@tukorea.ac.kr

time, and sintering temperature. The research seeks to optimize the mixing ratio of ITO and ATO to reduce financial burdens in display production processes, maintain electrical resistance properties, and address resource cost issues [21-24].

## 2. METHODOLOGY

In this study, colloidal solutions were prepared using a wet grinding method to manufacture transparent conductive coating layers via the electrospinning method. To prepare the spinning solution, ATO (Sigma Aldrich) and ITO nanopowder (KS Trading Co. Ltd.) were used as dispersed phases, and ethanol (Daejung Chemical, HPLC grade, 99.9 %) served as the dispersion medium. Acetylacetone (ACAC, 99.0 %, Junsei Chemical Co.) was used as dispersant to maintain the stability of the colloidal suspension. Acetylacetone is widely recognized as a bidentate ligand capable of effectively preventing aggregation by attaching to the surface of metal oxide particles. Additionally, titania (KR44) or silane-based like N-(2-Aminoethyl)-3dispersants aminopropyltrimethoxysilane (AAPTS, Sigma-Aldrich) were also adopted as dispersants [25]. Silane coupling agents with relatively small molecular weights can chemically adsorb onto ITO or ATO particles. Therefore, they are considered suitable choices for acting as dispersion stabilizers in ITO or ATO nano-colloids to obtain stable coating solutions.

For the preparation of the colloidal solution, a milling process involving mechanical impact using a vibratory tumbler, as depicted in Fig. 1 a, was conducted to reduce the size of nanoparticles within the dispersion. Zirconia beads (Ceratek.Inc, CZY0010, 0.1 mm in diameter) were used as grinding media for this purpose. The dispersant (0.3 g), selected from ACAC, KR44, or AAPTS, was mixed with 15.6 g of ethanol to prepare dispersant solution. To prepare the dispersion, 0.8 g of ITO or ATO powder, 6 mL of ethanol, 3 mL of zirconia beads, and 3.6 g of dispersant solution (chosen from ACAC, KR44, or AAPTS) were placed into a Nalgene bottle. The mixture was then subjected to mechanical agitation using a vibratory tumbler for 6 hours. As a result, the obtained colloidal dispersions were separated from the zirconia beads by gravity, and both ITO and ATO remained stable without aggregation for at least 3 weeks and up to 2 months.

The electrospinning method was employed for the fabrication of the transparent conductive coating layer, as presented schematically in Fig. 1 b. To form a Taylor cone during electrospinning using high-voltage power supply (Nano NC, YAH1225S2), the solution's viscosity needed to be sufficiently high [26]. Therefore, a solution was prepared by stirring 1 g of PVP (polyvinylpyrrolidone, Sigma-Aldrich, Mw = 360,000) in 7 mL of ethanol for more than 3 hours. Subsequently, a final solution for electrospinning was prepared by mixing 3 mL of the prepared ITO-ATO mixed spinning solution and 3 mL of PVP solution, according to specified chemical formulation conditions [24, 25]. The chemical formulation conditions included solutions with ITO content of 0, 10, 30, 50, 60, 70, 90, and 100 vol.%. Independent experiments were conducted using KR44, ACAC, and AAPTS dispersants for electrospinning.

Slide glass (25 mm  $\times$  75 mm) was used for collecting electrospun fibers for surface resistance measurements, and 25 mm  $\times$  25 mm pieces of 150 mm  $\times$  150 mm glass slides were used for optical transmittance measurements. All substrates used in the experiment were sequentially cleaned by ultrasound cleaner (Hwashin, POWER SONIC 405) for 10 minutes each with acetone (Samchun Chemicals, 99.5 %), methanol (Samchun Chemicals, 99.5 %), and isopropyl alcohol (Samchun Chemicals, 99.5 %), followed by drying. The electrospinning solution was injected into a syringe (HENKE-JECT, Luer) equipped with a 21-gauge needle. The distance between the needle tip and the glass substrate was set at 13.5 cm. Electrospinning was carried out under the following parameters: flow rate of 10 µL/min, voltage of 12 kV, humidity maintained at 30 to 35 %, and spinning times of 5, 10, 20, and 30 minutes were performed once each.

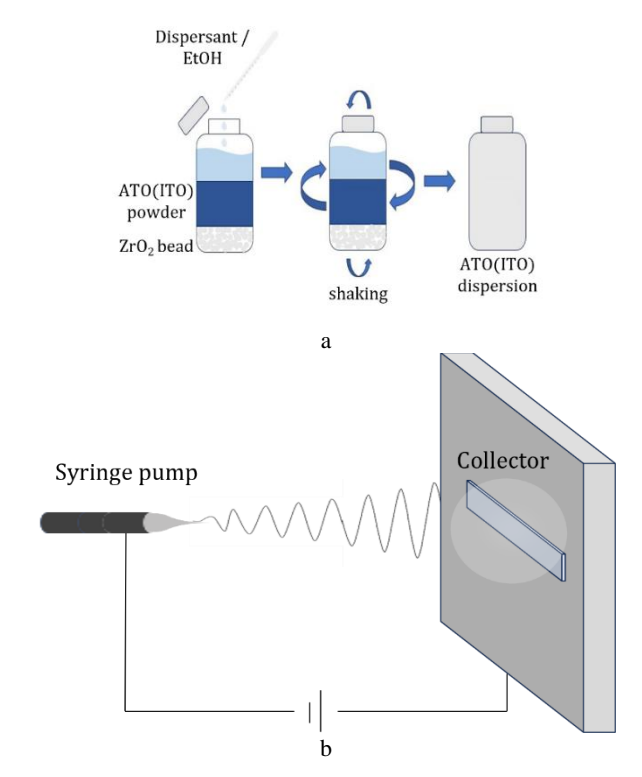


**Fig. 1.** a – preparation of colloidal solution using wet milling method; b – manufacturing of transparent conductive coating layers by electrospinning

After electrospinning, the glass substrates underwent annealing using an electric furnace (HANTECH Co., M-13P) at 500 °C for 13 hours under ambient conditions, with a ramp-up time of 8 hours and a dwell time of 5 hours. This process resulted in the formation of a transparent conductive coating layer on the glass substrates, as depicted in Fig. 2.

Surface resistance was estimated using the transmission line method (TLM), a method of calculating contact resistance using horizontal electrodes. After annealing, the sample was prepared with seven patterns using silver paste (CANS ELCOAT P-100) as shown in the Fig. 3 a, each with an equal spacing of 7 mm and a line width of 1 mm. Following a two-day drying period for the silver paste, resistance measurements were conducted. A multimeter was used to measure the contact resistance, with one probe fixed on the first electrode while the other probe was sequentially

moved from the second to the seventh electrode to measure the contact resistance.

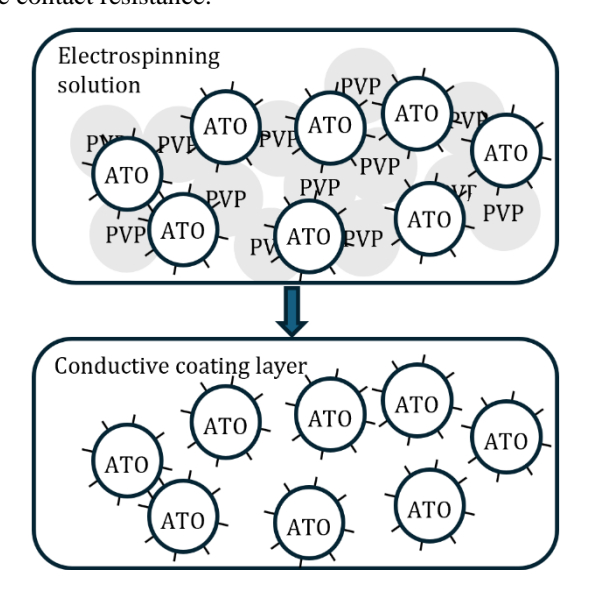
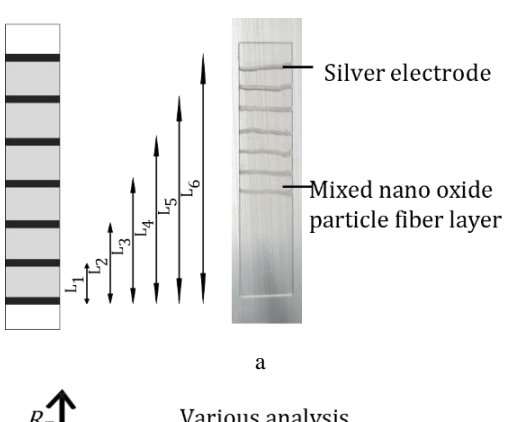


Fig. 2. Schematic diagram of the annealing process for nanofibercollected substrates



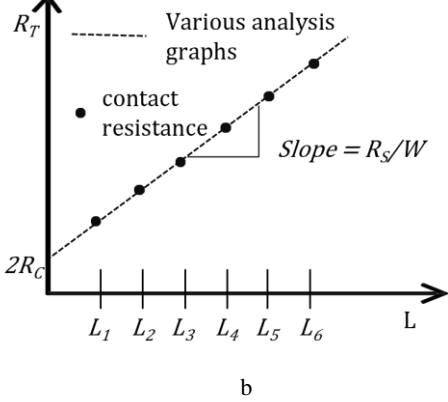


Fig. 3. a – surface resistance measurement by TLM method (left), Photograph of a sample coated with silver paste for surface resistance measurement (right); b–plots of regression analysis using contact resistance data to determine  $R_s$ 

The total resistance can be expressed by the following equation:

$$R_T = 2R_m + 2R_c + R_{semi},\tag{1}$$

where  $R_m$  is the resistance due to the contact metal;  $R_c$  is the resistance that occurs between the metal or semiconductor interface;  $R_{semi}$  is the bulk resistance. In most cases, the contact resistivity is very low, so  $R_m$  can be ignored. In this

case, the resistance of the semiconductor can be obtained from the following relationship.

$$R_{semi} = R_s \times \frac{L}{w}. (2)$$

And the total resistance can be calculated from the following equation.

$$R_T = \frac{R_S}{W}L + 2R_C,\tag{3}$$

where  $R_s$  is the sheet resistance; L is the length; W is the width [27].

Fig 3 a shows a typical configuration for TLM method. The silver paste was patterned at equal intervals of 7 mm. In this TLM method, the silver paste pattern used a width (W) of 25 mm and various lengths (L) of 7, 14, 21, 28, and 35 mm. Each measured contact resistance was used to construct a graph as shown in Fig. 3 b, and the  $R_s$  parameter representing the sheet resistance can be determined using the constructed regression line.

# 3. RESULTS AND DISCUSSION

Nano-colloids were obtained as stable dispersion through chemical adsorption of dispersing agent during milling process and their particle size distributions were measured according to three types of dispersants. As shown in Fig. 4, the size distribution of ITO and ATO nano-colloids prepared using AAPTS as a dispersant was measured using dynamic light scattering (DLS) during the milling process [28]. Aggregated particles were separated during the milling process, and stable dispersions were achieved after chemisorption of the silane coupling agent. The average particle sizes of ITO and ATO nano-colloids were measured as 112.7 and 124.0 nm, respectively, indicating that the nozzle did not clog during electrospinning.

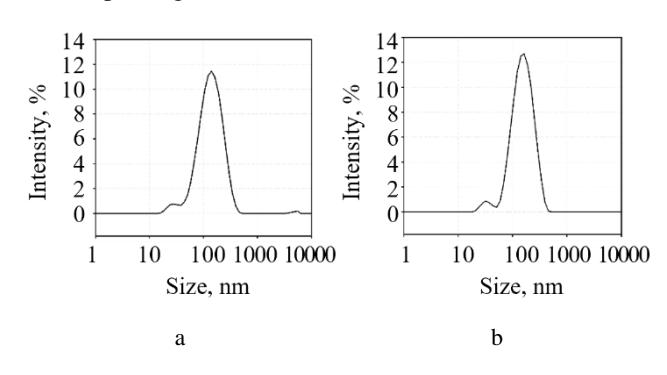


**Fig. 4.** Size distribution of secondary particles: a-ITO; b-ATO nanocolloids, respectively, using AAPTS as dispersant after vibratory milling for 6 hours

Similar to AAPTS, KR44 exhibited a comparable effect for dispersion stabilization of ITO and ATO nano-colloids, as shown in Fig. 5 a and b. After 6 hours of milling, the average diameters of the nano-colloids were measured to be 119.1 and 126.9 nm, respectively. The chemical adsorption of AAPTS and KR44 on the particle surfaces modified the oxide nanoparticles with amine-functionalized surface groups, thereby enhancing the dispersion stability of the particles in organic solvents. In addition to silane or titanate coupling agents, as shown in Fig. 5 c and d, acetyl acetone

was adopted as an efficient dispersant for preparing ITO and ATO nano-colloids. After milling for 6 hours, the average particle sizes were measured to be 118.1 and 126.7 nm, respectively.

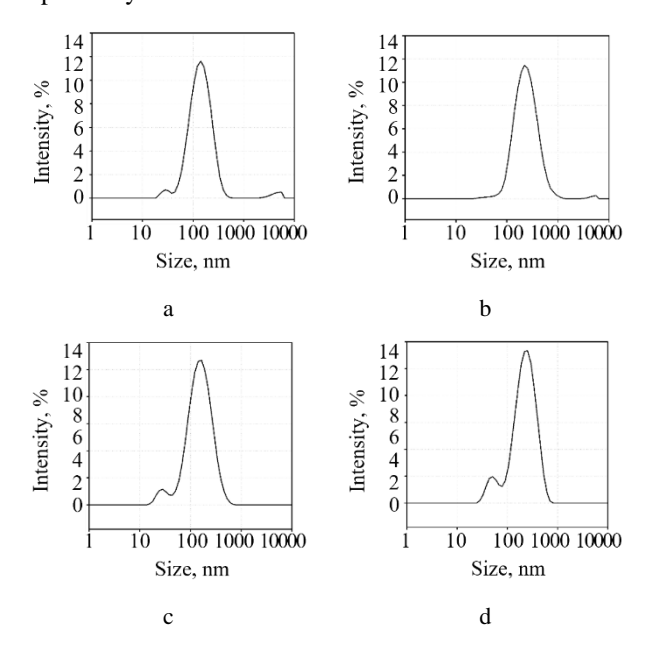
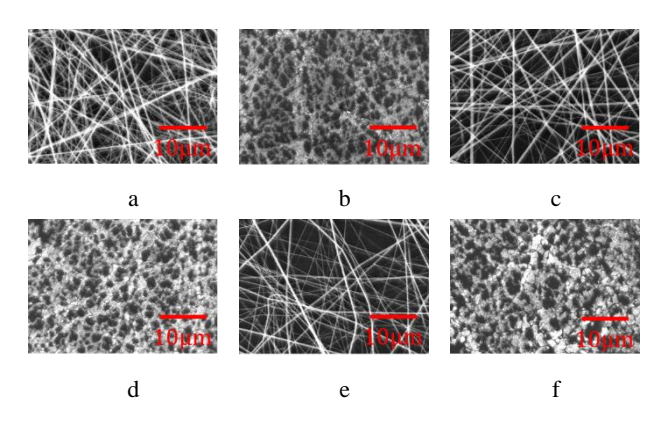


Fig. 5. Secondary particle size distributions: a-ITO and b-ATO nano-colloids using KR44 as a dispersant after 6 hours of vibratory milling; c-ITO and d-ATO nano-colloids using ACAC as a dispersant

Various mixtures of ITO and ATO nanoparticles colloidal dispersions were prepared for electrospinning onto glass substrates. These mixtures were formulated using different dispersants during the milling process to stabilize the nanoparticles. The morphology and uniformity of the electrospun fibers were analyzed using Scanning Electron Microscopy (SEM). Fig. 6, Fig. 7, and Fig. 8 contain SEM images of representative samples of electrospun fibers, highlighting the differences depending on the dispersants used during the milling process.



**Fig. 6.** SEM images of electrospun fibers of 1:1 mixed nano colloids of ITO and ATO: a, b-samples prepared with AAPTS; c, d-acetylacetone; e, f-KR44, before and after heat treatment at 500 °C. The scale bar represents 10 μm

After electrospinning, the fibers with uniform thickness could be generated from the conductive nanoparticles mixed with PVP. After calcination, fiber networks composed of nanoparticles could be fabricated by removal of organic components of PVP by heating. The images in Fig. 6–Fig. 8

reveal the impact of each dispersant on the fiber structure, distribution, and nanoparticle alignment within the fibers. Post-electrospinning, the fibers comprised a mixture of conductive nanoparticles and PVP. This mixture facilitated the formation of uniform fibers during the electrospinning process. Subsequent annealing was performed to remove the organic components of PVP through heating. The annealing process not only eliminated the PVP but also promoted the sintering of the nanoparticles, leading to the formation of a robust fiber network composed purely of conductive nanoparticles. This network structure is crucial for enhancing the electrical conductivity and mechanical stability of the fibers, making them suitable for various applications in electronics and material engineering.

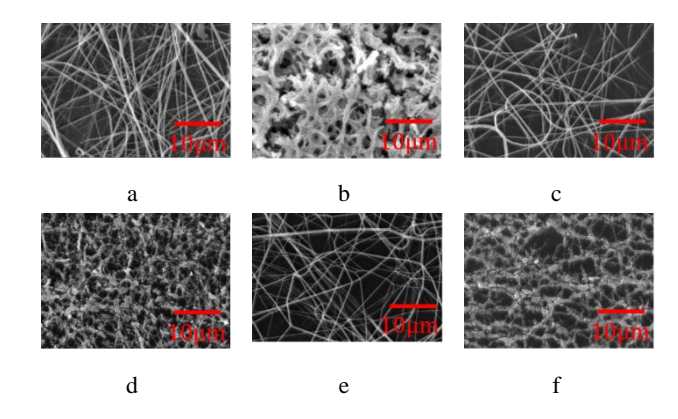


Fig. 7. SEM images of electrospun fibers of ATO nano colloids prepared with: a, b-AAPTS; c, d-acetylacetone; e, f-KR44, before and after heat treatment at 500 °C. The scale bar represents 10 μm

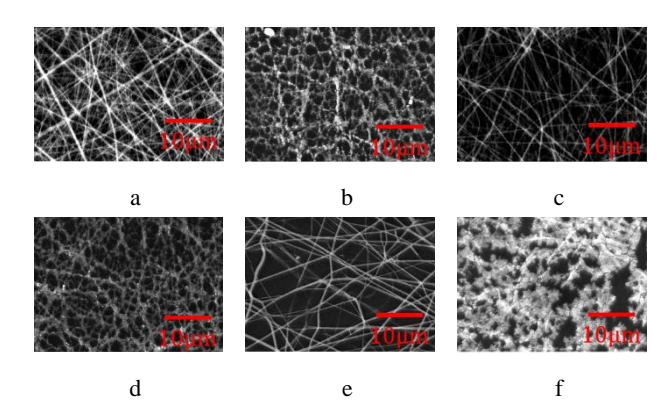
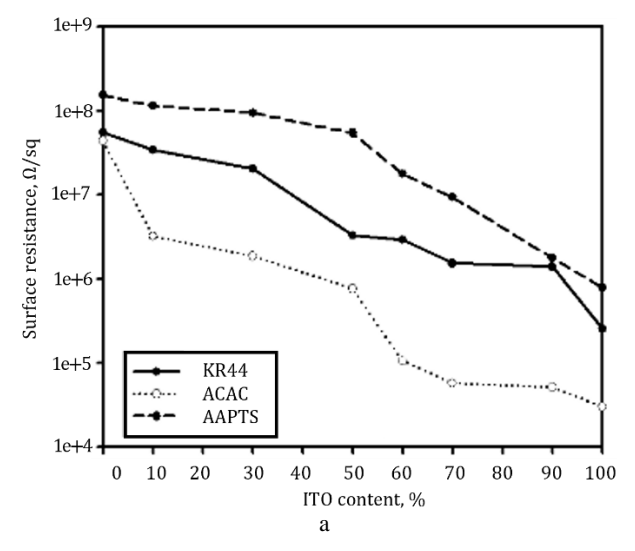
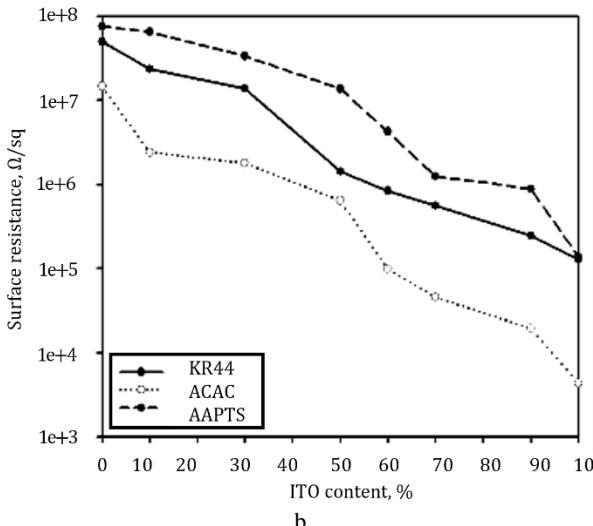
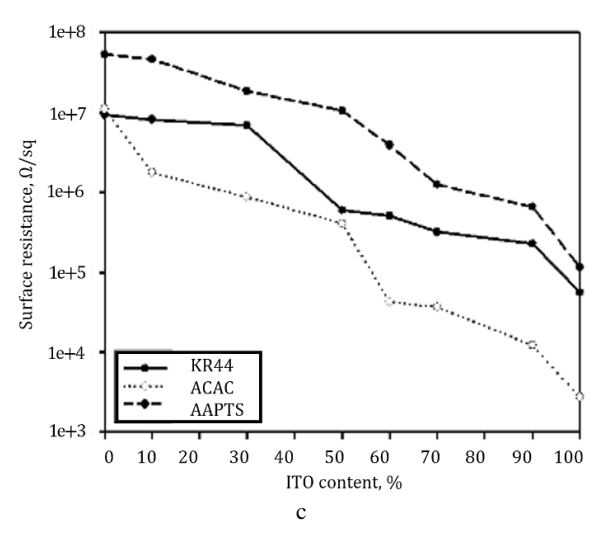


Fig. 8. SEM images of electrospun fibers of ITO nano-colloids prepared with: a, b-AAPTS; c, d-acetylacetone; e, f-KR44, before and after heat treatment at 500 °C. The scale bar represents 10  $\mu$ m

Fig. 9 shows the surface resistance of electrospun fibers composed of ITO and ATO nanoparticles stabilized with ACAC, AAPTS, and KR44 at various mixing ratios, plotted as a function of the mixing ratio. As the concentration of ITO nano-colloids increased, the surface resistance decreased regardless of the dispersants used [29]. This trend is attributed to the superior electrical conductivity of ITO compared to ATO [30]. Additionally, an experiment was conducted with the expectation that using ACAC, a dispersant that evaporates during the heat treatment process, would remove the insulating layer between the particles constituting the electrospun fibers, thus reducing resistance.







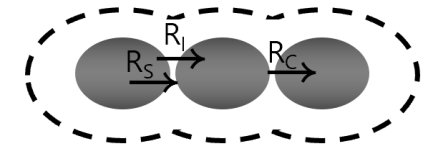
**Fig. 9.** Surface resistance of electrospun fibers of ITO and ATO nanoparticle mixtures as a function of the ratio of ITO with respect to: a – 10 min; b – 20 min; c – 30 minutes of electrospinning, using three different dispersants

Films coated with ACAC exhibited the lowest surface resistance, likely due to the complete removal of acetylacetone (boiling point: 140 °C) along with PVP during heat treatment at 500 °C. On the contrary, AAPTS and KR44 adsorb onto the nanoparticle surface, forming an

insulating layer that persists even after annealing, thereby increasing the surface resistance of the films. Fig. 10 is a schematic model illustrating the electrical resistance of ITO and ATO conductive transparent films. The resistance of this film arises from the resistance of the nanoparticles (specific resistance,  $R_S$ ), the resistance of the adsorbed surfactant layer (surface adsorption resistance,  $R_I$ ), and the contact resistance ( $R_C$ ). The total resistance ( $R_O$ ) of the coated film can be expressed by Eq. 4 [31].

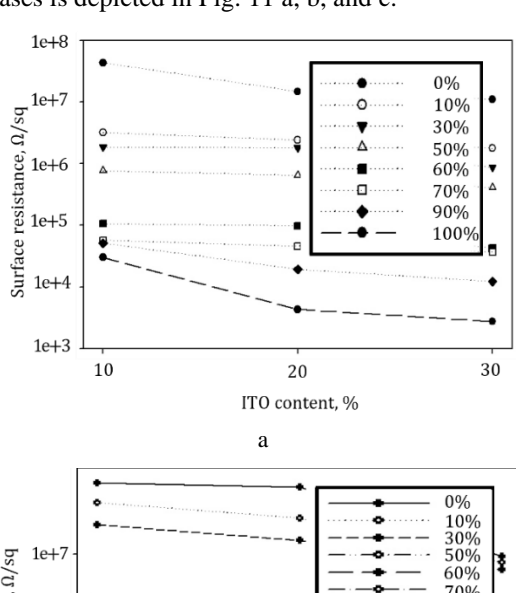
$$\frac{1}{R_O} = \frac{1}{R_S + R_C} + \frac{1}{R_I}.\tag{4}$$

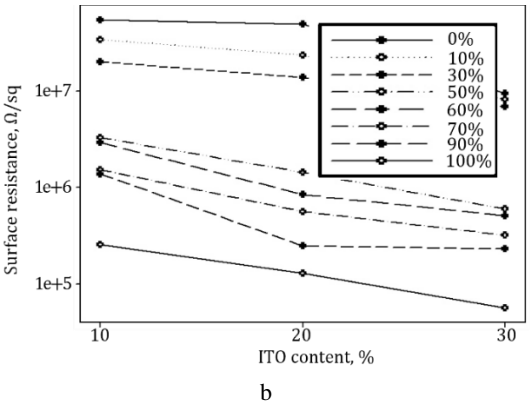
Because  $R_I$  can be neglected for the dispersion of ATO and ITO nanoparticles stabilized with ACAC, smaller surface resistance of electrospun fibers can be expected, as presented in dotted lines of Fig. 9. As a result, when the amount of ITO was larger than 40 % in the spinning solution, the surface resistance of the coating film was in the range of  $10^4 \Omega/\text{sq}$ , when spinning time was 30 minutes for the spinning solution obtained using ACAC as a dispersant, indicating that optimal mixing ratio in the spinning solution can be obtained from 30 to 40 % of ITO nanoparticles.



**Fig. 10.** Schematic diagram of a model for the electrical resistance of a conductive film

In this study, for the three types of dispersants, the change of surface resistance as a function of ITO content increases is depicted in Fig. 11 a, b, and c.





continued on the next page

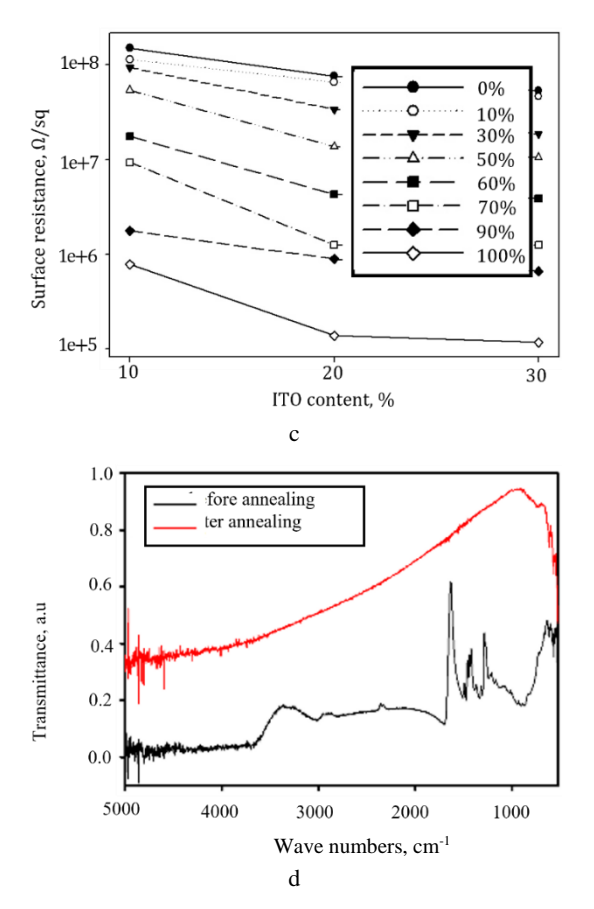
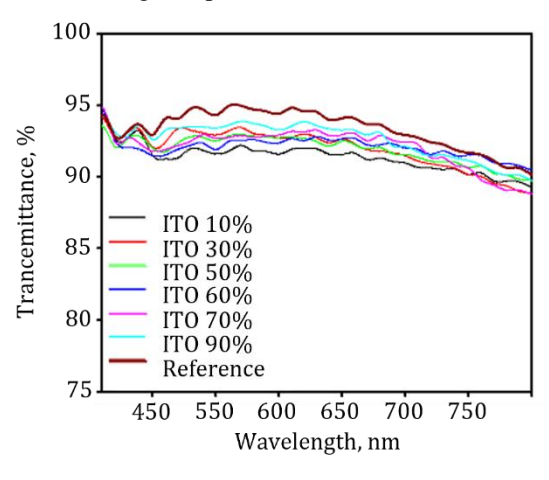


Fig. 11. Graph showing the surface resistance of electrospun fibers composed of various ratios of ITO and ATO mixed nano particles stabilized with: a−ACAC; b−AAPTS; c−KR44 over time; d−FT-IR spectra of elecrospun fibers of ITO and ATO nanoparticle mixture before and after heat treatment at 500 °C

As the electrospinning time increased, more conductive nanoparticles were deposited onto the substrate, resulting in a decrease in surface resistance. While the results were not consistent across all dispersants, an overall trend was observed where the surface resistance of the coated films decreased with increasing electrospinning time. This is attributed to the increased deposition of conductive nanoparticles as the electrospinning time increases. This reduction in surface resistance with electrospinning time underscores the importance of optimizing electrospinning parameters to achieve desired electrical properties in nanofiber films. As presented in Fig. 11 d, miscellaneous peaks originated from PVP disappeared after calcination, implying that 500 °C is a sufficient temperature for the removal of polymeric additives in the spinning solution [32].

In Fig. 12, visible light spectra of coating films were compared with reference sample (bare glass). Regardless of the amount of ITO in the spinning solution, the transmittance was higher than 90 % for most wavelength of incident light, showing excellent transparency. Thus, it can be concluded that the conductive transparent thin film is not significantly affected by the composition of the constituent solution. Although the results were not reproduced here, similar optical spectra were obtained from electrospun films prepared using other types of dispersants. FT-IR analyses of electrospun fibers of ITO and ATO nanoparticle mixture

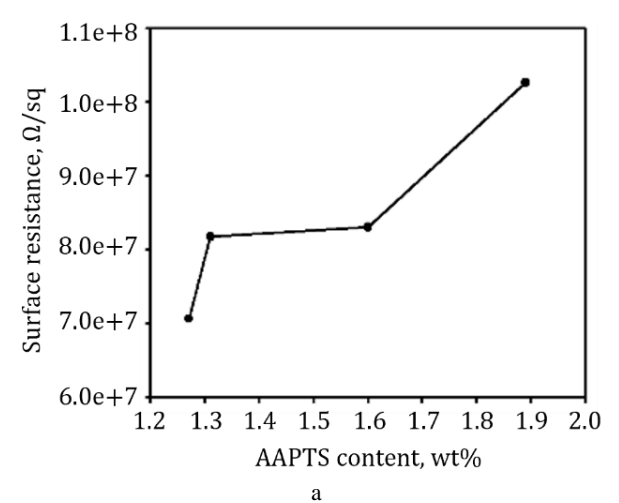
(1:1) were obtained for samples before and after heat treatment at 500 °C. There are various methods for TCO (Transparent Conductive Oxide) coating, including dip coating, spin coating, and spray coating, among these methods, electrospinning is suitable for mass production using multi-nozzle or needleless electrospinning, as minimal human intervention is required once the environment is established [33, 34]. Additionally, nanofiber coatings made by electrospinning are expected to improve optical transmittance, as they allow light to pass through gaps, unlike other coating methods. In fact, it has been shown that the optical transmittance was higher than that of conductive thin films produced by previously performed electrospinning and dip coating [35, 36]. Furthermore, compared to the previously conducted ATO (Antimony Tin Oxide) coating using electrospinning, an increase in optical transmittance were observed [37]. The additional advantage could be obtained by mixing of ITO with ATO, which reduced the resistance compared to the coating layer made by spinning for the same duration. The rapid increase in resistance was caused by shorter spinning times, which in turn resulted in higher optical transmittance.



**Fig. 12.** Visible light transmittance of electrospun coating films with various mixing ratios of ITO and ATO nanoparticles stabilized with ACAC

Fig. 13 depicts the surface resistance of conductive transparent coating layers manufactured via spin coating. In Fig. 13 a, it can be observed that with AAPTS, even after the sintering process, it permanently resides on the surfaces of ITO and ATO particles, leading to an increase in surface resistance with higher concentrations. Additionally, Fig. 13 b shows that regardless of the method used, an increase in the amount of ITO led to a decrease in surface resistance during the production of conductive transparent films. Because of a larger number of contacts between conductive nanoparticles in spin coating layer, surface resistance was measured from the spin-coated films as relatively larger values, compared to the results from electro-spun fibers.

As shown in Fig. 14, the surface resistance of the electrospun fibers (ITO 60 %) decreased by heating at 400 to 550  $^{\circ}$ C [38]. However, the surface resistance increased then the annealing temperature increased from 550 to 600  $^{\circ}$ C. This phenomenon is related to the glass transition temperature of the glass substrate used in the experiment, which is approximately 600  $^{\circ}$ C.



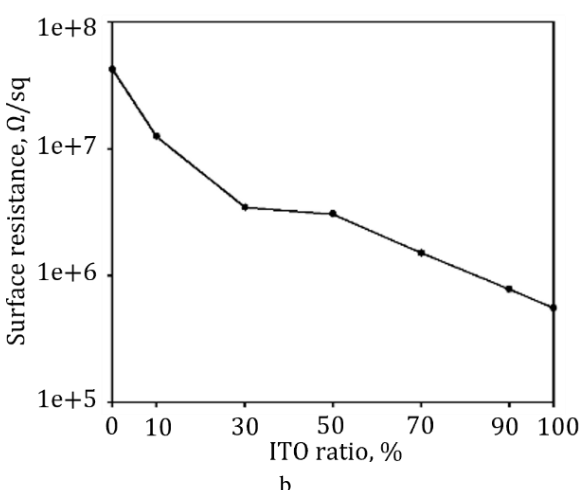
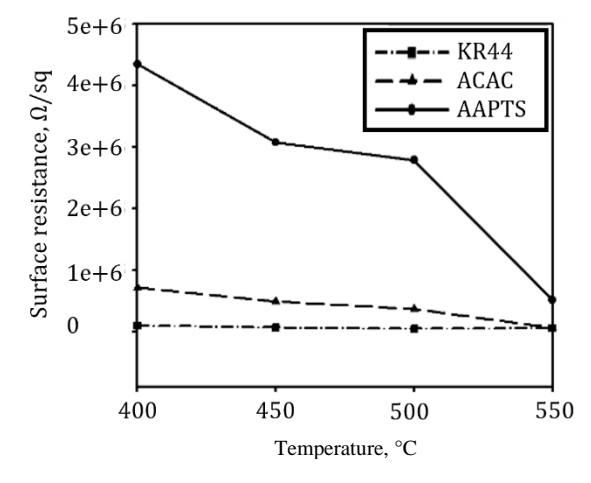


Fig. 13. a – surface resistance of conductive transparent coating layers of ATO manufactured using spin coating at varying concentrations of AAPTS; b – surface resistance of conductive transparent coating layers of ITO prepared using ACAC dispersant with varying mixing ratios



**Fig. 14.** Surface resistance of electrospun coating layers (ITO 60 %) for various dispersants, as a function of annealing temperature

At this temperature, deformation of the glass substrate likely caused damage to the transparent conductive coating layer, resulting in increased resistance. This indicates that the observed increase in resistance was due to deformation and subsequent damage to the coating layer. Conversely, the reason for the gradual decrease in resistance of the

conductive transparent coating layer from 400 to 550 °C is attributed to the consolidation of the ITO and ATO nanopowder as well as the enhanced removal of PVP through annealing at the elevated temperatures.

# 4. CONCLUSIONS

The colloidal dispersion of ATO and ITO nanoparticles as well as their mixed colloids were prepared by wetattrition process for electrospinning of the conductive nanoparticles on glass substrates. Because the particle size distribution in the dispersion showed no significant differences, it appears that the factors influencing the reduction of resistance in the conductive film are the type of dispersant used, the sintering temperature, and the spinning time. Despite varying the spinning time to 5, 10, 20, and 30 minutes, no significant changes in optical transmittance were observed. This suggests that the electrospun nanoparticles of ITO and ATO revealed sufficient optical transparency in the visible light region.

The surface resistance of conductive transparent coating layers decreases in the order of dispersants AAPTS, KR44, and ACAC. This is because ACAC is completely removed from the surfaces of ITO and ATO powders during the sintering process, whereas KR44 and AAPTS remain to some extent on the particle surfaces, thereby increasing the resistance.

During the sintering process, examining the relationship between 400 and 550 °C indicated that higher sintering temperatures, which facilitate greater removal of the organic components, led to lower surface resistance. Additionally, substrates that remain stable at high temperatures is expected to further reduce surface resistance of the electrospun nanoparticles.

The TCO coating method using multi-nozzle or needleless electrospinning is known to be suitable for mass production and requires minimal human intervention. Nanofiber coatings produced by electrospinning provide paths through which light can pass, leading to higher transmittance compared to other coating methods. It showed higher light transmittance than conductive films produced by electrospray and dip coating methods, and a reduction in resistance and an increase in transmittance were also observed compared to ATO coatings. This is interpreted as the result of mixing ITO, which allowed for lower resistance in the same spinning time, thereby enhancing the transmittance.

Increasing the electrospinning time resulted in a decrease in the resistance of the conductive film. This is because the electrospun fibers formed a more complex network as the spinning time increased, allowing more deposition of conductive nanoparticles.

To enhance the cost-effectiveness of ITO, the minimum amount of ITO that can be mixed is determined as 40 %. When the amount of ITO was larger than 40 % in the spinning solution, the surface resistance of the coating film was in the range of  $10^4 \, \Omega/\text{sq}$ , when the spinning time was 30 minutes.

The results of this study aim to address the cost issues associated with the production of conductive transparent films. By developing a technology for manufacturing ITO and ATO transparent conductive films, even after new

substitute materials are developed, this technology can be integrated with those materials. This integration will allow for the mass production of displays that not only exhibit increased cost benefits but also advantage from reduced reliance on new materials alone. Consequently, it is anticipated that this will lead to the production of more cost-effective products, thereby increasing market share and providing a competitive edge in the industry.

## Acknowledgments

This research was supported by the Priority Research Centers Program through the National Research Foundation of Korea (NRF), funded by the Ministry of Education [NRF-2017R1A6A1A03015562], a Research Foundation of Korea (NRF) grant, funded by the Korea government (MSIT) [No. RS-2023-00250648], and the Korea Institute of Energy Technology Evaluation and Planning(KETEP) grant funded by the Korea government(MOTIE) [20214000000090, Fostering human resources training in advanced hydrogen energy industry].

### REFERENCES

- Kim, E.H., Yang, C.W., Park, J.W. The Crystallinity and Mechanical Properties of Indium Tin Oxide Coatings on Polymer Substrates *Journal of Applied Physics* 109 (4) 2011: pp. 043511-043511. https://doi.org/10.1063/1.3559264
- Aleksandrova, M., Kurtev, N., Videkov, V., Tzanova, S., Schintke, S. Material Alternative to ITO for Transparent Conductive Electrode in Flexible Display and Photovoltaic Devices Microelectronic Engineering 145 (1) 2015: 112–116. https://doi.org/10.1016/j.mee.2015.03.053
- 3. **Montero, J., Herrero, J., Guillén, C**. Preparation of Reactively Sputtered Sb-doped SnO<sub>2</sub> Thin Films: Structural, Electrical and Optical Properties *Solar Energy Materials and Solar Cells* 94 (3) 2010: pp. 612–616. https://doi.org/10.1016/j.solmat.2009.12.008
- Boltz, J., Koehl, D., Wuttig, M. Low Temperature Sputter Deposition of SnO<sub>x</sub>: Sb Films for Transparent Conducting Oxide Applications Surface and Coatings Technology 205 (7) 2010: pp. 2455–2460. https://doi.org/10.1016/j.surfcoat.2010.09.048
- Batzill, M., Diebold, U. The Surface and Materials Science of Tin Oxide *Progress in Surface Science* 79 (2-4) 2005: pp. 47 154. https://doi.org/10.1016/j.progsurf.2005.09.002
- Santos-Pena, J., Herrero, J., Gonzalez-Bermudez, J., Pardo-Batuje, A. Antimony Doping Effect on the Electrochemical Behavior of SnO<sub>2</sub> Thin Film Electrodes *Journal of Power Sources* 97 2001: pp. 232 234. https://doi.org/10.1016/S0378-7753(01)00620-6
- Shokr, E.Kh., Abd-El-Kader, F.H., Abdallah, S., Soliman, M. Sb-Doping Effects on Optical and Electrical Parameters of SnO<sub>2</sub> Films *Journal of Physics and Chemistry of Solids* 61 (1) 2000: pp. 75–85. https://doi.org/10.1016/S0022-3697(99)00234-6
- 8. Ostermann, R., Zieba, R., Rudolph, M., Schlettwein, D., Smarsly, B.M. Electrospun Antimony Doped Tin Oxide (ATO) Nanofibers as a Versatile Conducting Matrix *Chemical Communications* 47 2011: pp. 12119–12121. https://doi.org/10.1039/C1CC13724G

- Körber, C., Ágoston, P., Klein, A. Surface and Bulk Properties of Sputter Deposited Undoped and Sb-Doped SnO<sub>2</sub>
   Thin Films Sensors and Actuators B: Chemical 139 (2) 2009: pp. 665 672.
   https://doi.org/10.1016/j.snb.2009.03.067
- 10. **Kumar, D., Sharma, R.C.** Advances in Conductive Polymers *European Polymer Journal* 34 (8) 1988: pp. 1053 1060. https://doi.org/10.1016/S0014-3057(97)00204-8
- 11. **Angmo, D., Krebs, F.C**. Flexible ITO-Free Polymer Solar Cells *Journal of Applied Polymer Science* 129 (1) 2013: pp. 1–14. https://doi.org/10.1002/app.38854
- 12. **Popov, V.N.** Carbon Nanotubes: Properties and Application *Materials Science and Engineering: R: Reports* 43 (3) 2004: pp. 61 102. https://doi.org/10.1016/j.mser.2003.10.001
- 13. **De Volder, M.F.L.,** Tawfick, S.H., Baughman, R.H., Hart, A.J. Carbon Nanotubes: Present and Future Commercial Applications *Science* 339 (6119) 2013: pp. 535 539. https://doi.org/10.1126/science.1222453
- 14. **Li, D., Mishra, S.R., Huang, L.,** Mannsfeld, S.C.B. Printable Transparent Conductive Films for Flexible Electronics Advanced Materials 30 (10) 2018: pp. 1704738. https://doi.org/10.1002/adma.201704738
- Ma, Y., Zhi, L. Graphene-Based Transparent Conductive Films: Material Systems, Preparation and Applications *Small Methods* 3 (1) 2019: pp. 1800199. https://doi.org/10.1002/smtd.201800199
- Singh, D., Tao, R., Lubineau, G. A Synergetic Layered Inorganic–Organic Hybrid Film for Conductive, Flexible, and Transparent Electrodes *npj Flexible Electronics* 3 (10) 2019: pp. 1–8. https://doi.org/10.1038/s41528-019-0054-4
- 17. Yang, B., Jia, Y., Li, S., Wang, L., Zhou, J. Nature Degradable, Flexible, and Transparent Conductive Substrates from Green and Earth-Abundant Materials *Scientific Reports* 7 (1) 2017: pp. 4936. https://doi.org/10.1038/s41598-017-04969-y
- 18. **Minami, T.** Present Status of Transparent Conducting Oxide Thin-Film Development for Indium-Tin-Oxide (ITO) Substitutes *Thin Solid Films* 516 (17) 2008: pp. 5822 5828. https://doi.org/10.1016/j.tsf.2007.10.063
- Najafi, M., Ghanbari, S., Sundararaj, U., Park, C.B. Biodegradable Polylactic acid Emulsion Ink based on Carbon Nanotubes and Silver for Printed Pressure Sensors Scientific Reports 14 (1) 2024: pp. 10988. https://doi.org/10.1038/s41598-024-60315-z
- Yu, L.P., Shearer, C., Shapter, J. Recent Development of Carbon Nanotube Transparent Conductive Films *Chemical Reviews* 116 (22) 2016: pp. 13413 – 13453. https://doi.org/10.1021/acs.chemrev.6b00179
- 21. **Shanthi, E., Banerjee, A., Rangaraju, R., Sivaramakrishnan, R.** Electrical and Optical Properties of Undoped and Antimony-Doped Tin Oxide Films *Journal of Applied Physics* 51 (12) 1980: pp. 6243–6251. https://doi.org/10.1063/1.327610
- 22. **Kim, H., Piqué, A., Horwitz, J.S., Mattoussi, H., Murata, H., Kafafi, Z.H., Chrisey, D.B.** Indium Tin Oxide
  Thin Films for Organic Light-Emitting Devices *Applied Physics Letters* 74 (23) 1999: pp. 3444–3446. https://doi.org/10.1063/1.124122

- Mierzwa, M., Lamouroux, E., Vakulko, I., Durand, P., Etienne, M. Electrochemistry and Spectroelectrochemistry with Electrospun Indium Tin Oxide Nanofibers Electrochimica Acta 202 2016: pp. 55 65. https://doi.org/10.1016/j.electacta.2016.03.136
- 24. Cho, Y.S., Han, M., Woo, S.H. Electrospinning of Antimony Doped Tin Oxide Nanoparticle Dispersion for Transparent and Conductive Films Archives of Metallurgy and Materials 65 (4) 2020: pp. 1351–1358. https://doi.org/10.24425/amm.2020.133681
- Nguyen, H.H., Tran, Q.H., Kim, Y.S., Cho, Y.S. Fabrication of Functional Coating Layer for Emerging Transparent Electrodes Using Antimony Tin Oxide Aano-Colloid *Materials Science* 14 (4) 2024: pp. 987–995. https://doi.org/10.5755/j02.ms.34452
- Hegab, H., Tariq, M., Syed, N.A., Rizvi, G., Pop-Iliev, R. Towards Analysis and Optimization of Electrospun PVP (polyvinylpyrrolidone) Nanofibers Advances in Polymer Technology 2020 (1) 2020: pp. 4090747. https://doi.org/10.1155/2020/4090747
- 27. **Grover, S., Sahu, S., Zhang, P., Davis, K. O., Kurinec, S.K.** Standardization of Specific Contact Resistivity Measurements Using Transmission Line Model (TLM) *International Conference on Microelectronic Test Structures* 2020 (33) 2020: pp. 1–6. https://doi.org/10.1109/ICMTS48187.2020.9107911
- 28. Kaszuba, M., McKnight, D., Connah, M.T., McNeil-Watson, F.K., Nobbmann, U. Measuring Sub Nanometre Sizes Using Dynamic Light Scattering Journal of Nanoparticle Research 10 2008: pp. 823–829. https://doi.org/10.1007/s11051-007-9317-4
- Song, I.S., Heo, S.W., Lee, J.H., Haw, J.R., Moon, D.K. Study on the Wet Processable Antimony Tin Oxide (ATO) Transparent Electrode for PLEDs *Journal of Industrial and Engineering Chemistry* 18 2012: pp. 312–316. https://doi.org/10.1016/j.jiec.2011.11.051
- 30. **Bisht, H., Eun, H.T., Mehrtens, A., Aegerter, M.A.,** Comparison of Spray Pyrolyzed FTO, ATO and ITO Coatings for Flat and Bent Glass Substrates *Thin Solid Films* 351 (1–2) 1999: pp. 109–114. https://doi.org/10.1016/S0040-6090(99)00254-0
- 31. Cho, Y.S., Yi, G.R., Hong, J.J., Jang, S.H., Yang, S.M. Colloidal Indium Tin Oxide Nanoparticles for Transparent

- and Conductive Films *Thin Solid Films* 515 (4) 2006: pp. 1864 1871. https://doi.org/10.1016/j.tsf.2006.07.022
- 32. Mondal, D., Mollick, M.M.R., Bhowmick, B., Maity, D., Bain, M.K., Rana, D., Mukhopadhyay, A., Dana, K., Chattopadhyay, D. Effect of Poly(vinyl pyrrolidone) on the Morphology and Physical Properties of Poly(vinyl alcohol)/Sodium Montmorillonite Nanocomposite Films *Progress in Natural Science: Materials International* 23 2013: pp. 579 587. https://doi.org/10.1016/j.pnsc.2013.11.009
- 33. **Wei, L., Sun, R., Liu, C., Xiong, J., Qin, X.** Mass Production of Nanofibers from Needleless Electrospinning by a Novel Annular Spinneret *Materials and Design* 179 2019: pp. 107885. https://doi.org/10.1016/j.matdes.2019.107885
- 34. Jiang, J., Zheng, G., Wang, X., Li, W., Kang, G., Chen, H., Guo, S., Liu, J. Arced Multi-Nozzle Electrospinning Spinneret for High-Throughput Production of Nanofibers *Micromachines* 11 2020: pp. 27. https://doi.org/10.3390/mi11010027
- 35. **Goebbert, C., Nonninger, R., Aegerter, M.A., Schmidt, H.**Wet Chemical Deposition of ATO and ITO Coatings Using Crystalline Nanoparticles Redispersable in Solutions *Thin Solid Films* 351 1999: pp. 79 84. https://doi.org/10.1016/S0040-6090(99)00209-6
- Cho, Y.S., Jeong, S., Nam, S. Stable Dispersion of ITO Nanoparticles for Self-Organization by Electrospinning and Electrospray *Journal of Dispersion Science and Technology* 41 (13) 2020: pp. 1963–1975. https://doi.org/10.1080/01932691.2019.1645023
- 37. **An, H.R., Koo, B.R., Ahn, H.J., Lee, T.K.** Electrical and Optical Properties of Sb-Doped SnO<sub>2</sub> Transparent Conductive Films Fabricated by Using Electrospinning *Korean Journal of Materials Research* 25 (4) 2015: pp. 177 182. http://dx.doi.org/10.3740/MRSK.2015.25.4.177
- 38. **Ahmed, M., Bakry, A., Qasem, A., Dalir, H.** The Main Role of Thermal Annealing in Controlling the Structural and Optical Properties of ITO Thin Film Layer *Optical Materials* 113 2021: pp. 110866. https://doi.org/10.1016/j.optmat.2021.110866



© Lee et al. 2025 Open Access This article is distributed under the terms of the Creative Commons Attribution 4.0 International License (http://creativecommons.org/licenses/by/4.0/), which permits unrestricted use, distribution, and reproduction in any medium, provided you give appropriate credit to the original author(s) and the source, provide a link to the Creative Commons license, and indicate if changes were made.